MAGNETOHYDRODYNAMICS Vol. 58 (2022), No. 4, pp. 379–387
DOI: 10.22364/mhd.58.4.1

MAGNETIC FIN FOR HEAT TRANSFER ENHANCEMENT IN LIQUID METAL DUCT FLOW

Verónica Solano-Olivares[1], *Sergio Cuevas*[1], *Aldo Figueroa*[2]

[1] *Instituto de Energías Renovables, Universidad Nacional Autónoma de México, A.P. 34, Temixco, Morelos 62580, México*
[2] *CONACYT-Centro de Investigación en Ciencias, Universidad Autónoma del Estado de Morelos, Cuernavaca, Morelos 62209, México*

The use of fins in heat exchangers is one of the most common procedures to promote heat transfer enhancement. Here, we explore numerically the effect of a non-intrusive electromagnetic method, namely, a *magnetic fin*, to enhance heat transfer in a liquid metal duct flow. The idea is to place a small-size magnet externally to the duct but close to a heated wall so that the Lorentz force created in the fluid by the interaction of the induced electric currents and the localized magnetic field brakes the liquid metal flow creating vorticity and improving the convective heat transfer. Thus, the action of the localized Lorentz force (i.e. the magnetic fin) is analogous to the surface force created by a solid fin. Focusing the attention on how the laminar bulk flow affected by the presence of a magnetic fin influences the heat transfer on a heated sidewall in a wide interval of Hartmann numbers ($0 \leq \mathrm{Ha} \leq 550$) for fixed Reynolds numbers ($\mathrm{Re} = 500,1000,1500$), a two-dimensional numerical approximation is implemented. Optimal values for heat transfer enhancement of the interaction parameter $\mathrm{N} = \mathrm{Ha}^2/\mathrm{Re}$ and magnet–wall separation are determined as well as the percentage increment of heat transfer due to the presence of the magnetic fin.

Introduction.

Many technological applications rely on the optimal performance of heat exchangers, so having reliable methods of improving heat transfer becomes of paramount importance. We can distinguish between active methods that require external power, and passive methods that require no external power. Due to practical and economic reasons, passive methods are usually preferred in many applications. With these methods, the heat transfer rate is increased by promoting changes in the flow pattern, for instance, by inserting swirl devices that lead to the enhancement of the convective heat transfer and to the increase of the pressure drop. In most common heat exchangers, these devices can be surface or geometrical modifications that promote swirl into the bulk flow while disrupting the boundary layer at the walls. The appearance of vortex motion may increase the heat transfer coefficient and consequently the Nusselt number [1].

One of the most common strategies to enhance the heat transfer is by placing solid obstacles in the flow region. In particular, the use of extended surfaces like fins is widely employed with the aim of generating swirl and eventually turbulence. But mechanical methods are not the only option to promote vortex motion when electrically conducting fluids such as liquid metals come into play. Due to its high thermal conductivity, liquid metals under magnetic fields offer an alternative to the usual hydrodynamic flows in many technological applications, particularly, for cooling and heat transfer enhancement purposes, as occurs in metallurgical operations and coolant systems of fusion reactors. In fact, flows around solid obstacles have been investigated with the purpose of improving the heat transfer in MHD channel flows under a uniform magnetic field [2]. Other studies have explored active methods, for instance, by injecting a non-uniform electric current through electrodes under a uniform magnetic field [3]. A combination of pass-

ive and active methods has been also analysed to enhance the heat transfer from the heated sidewall of an MHD duct under a uniform magnetic field by using a cylinder wake mechanism augmented with a current injection forcing that enhances instability behind the cylinder [4]. In turn, the effects on the convective heat transfer of non-uniform magnetic fields have been investigated in a liquid metal flow in a parallel plate channel, where electric currents positioned underneath the channel walls created a "magnetic-ribs" distribution [5]. Actually, the heat transfer in liquid metal duct flows can be enhanced without solid obstacles or injected currents by the use of localized magnetic fields created by permanent magnets, which gives rise to magnetic obstacles [6]. In fact, the Lorentz force produced in the fluid by the interaction of the induced electric currents and the localized magnetic field brakes the liquid metal and creates vortical flows that improve the convective heat transfer. Here, we explore numerically the use of this non-intrusive electromagnetic method to promote heat transfer enhancement in liquid metal flows in ducts using localized magnetic fields near the heated wall but externally to the duct, what we named *magnetic fins*. Although some previous works have investigated the influence on heat transfer of one central magnetic obstacle [7] or a row of magnetic obstacles [8] in a duct flow, only a few values of the interaction parameter and Reynolds number were examined. In this contribution, with the aim of exploring a broad range of parameters, where a transition among a variety of flow patterns created by the magnetic fin is displayed, we restricted our attention to the laminar bulk flow exterior to the Hartmann and viscous layers approximating it as two-dimensional, and analyse its influence on the heat transfer on the heated sidewall. In addition, the effect of the magnet–wall separation from the heated wall which is assumed to be electrically conducting is considered.

1. Formulation.

We analyse numerically the flow and heat transfer of a viscous, incompressible, electrically conducting fluid in a rectangular duct under the field produced by a rectangular permanent magnet located underneath the duct and close to a heated sidewall, as shown in Fig. 1. Since the Hartmann and viscous layers near horizontal walls have a minor influence on the heat transfer and the largest temperature gradients are in the transversal direction to the heated sidewall, we approximate the flow as two-dimensional to focus attention on the impact of the laminar bulk flow on the heat transfer.

In dimensionless units, the sides of the rectangular magnet are $M_x = 1$ and $M_y = 2$. Considering the side length of the magnet in the x-direction as the characteristic length L_c, the duct length is $L_x = 50$ and the distance between side walls is $L_y = 14$.

The side wall at $y = 0$ (the heated wall) is set at a uniform temperature that is higher than the fluid inlet temperature. This wall is assumed to be of perfect electrical conductivity, whereas the opposing wall at $y = L_y$ is electrically insulating and adiabatic. The separation distance between the magnet and the heated wall is G. We carry out this study with a fixed blockage ratio $\beta = M_y/L_y = 1/7$ and different gap ratios $h = G/M_y$ in the range $0.05 < h < 0.45$, while the location of the magnet in the x coordinate remains fixed at $x = 12$. The field distribution of the permanent magnet was modelled using analytical expressions provided by Furlani [9].

The governing equations expressed in dimensionless form under the low magnetic Reynolds number approximation are

$$\nabla \cdot \mathbf{u} = 0, \tag{1}$$

$$\frac{\partial \mathbf{u}}{\partial t} + (\mathbf{u} \cdot \nabla)\,\mathbf{u} = -\nabla P + \frac{1}{\mathrm{Re}}\nabla^2 \mathbf{u} + \mathrm{N}(\mathbf{J} \times \mathbf{B}_0), \tag{2}$$

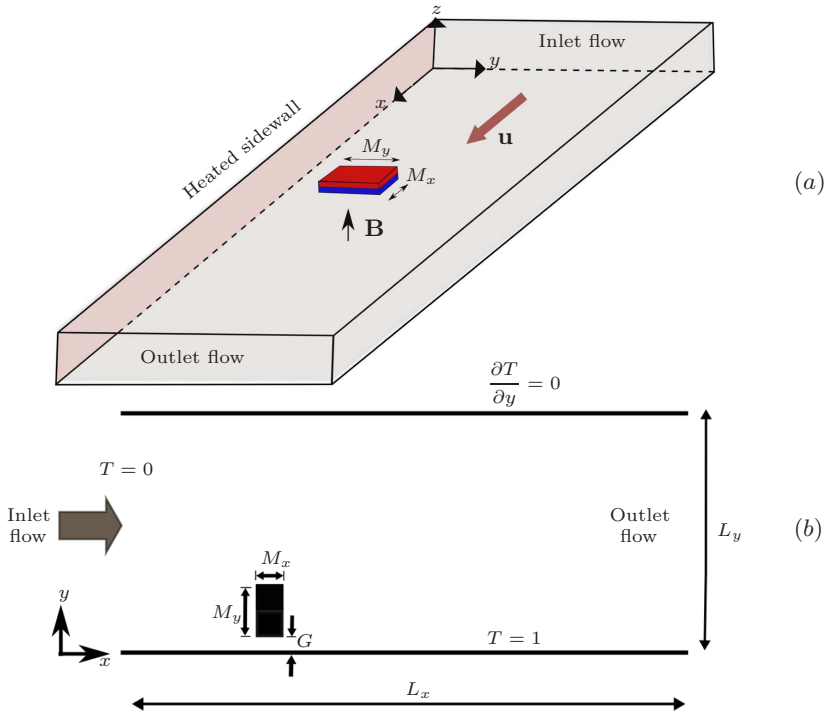

Fig. 1. Sketch of the analysed flow region.

$$\frac{\partial T}{\partial t} + (\mathbf{u} \cdot \nabla)\, T = \frac{1}{\mathrm{Pe}} \nabla^2 T, \tag{3}$$

$$\nabla^2 \mathbf{b} = (\mathbf{u} \cdot \nabla)\mathbf{B}_0, \tag{4}$$

$$\nabla \times \mathbf{b} = \mathbf{J}, \tag{5}$$

$$\nabla \cdot \mathbf{b} = 0, \tag{6}$$

where the velocity $\mathbf{u}$, pressure P, electric current density $\mathbf{J}$, applied magnetic field $\mathbf{B}_0$, and the induced magnetic field $\mathbf{b}$ have been normalized by U, ρU^2, $\sigma U B_{\max}$, $B_{\max}$, and $\mathrm{Rm} B_{\max}$, respectively, where U is the entrance velocity of the flow, and $B_{\max}$ is the maximum magnetic field strength of the permanent magnet, while ρ and σ are the mass density and the electrical conductivity of the liquid. Temperature is normalized as $(T' - T_0)/(T_1 - T_0)$, where T' is the dimensional fluid temperature and T_0 and T_1 are the fluid inlet temperature and the heated wall temperature, accordingly. $\mathrm{Rm} = \mu_0 \sigma U L_\mathrm{c}$ stands for the magnetic Reynolds number, where μ_0 is the magnetic permittivity of vacuum. The coordinates x, y, and the time t are normalized by L_c and L_c/U, respectively. The Galinstan alloy is chosen as a working fluid, whose Prandtl number is $\mathrm{Pr} = 0.053$. The dimensionless parameters are the Reynolds number $\mathrm{Re} = U L_\mathrm{c}/\nu$, the interaction parameter $\mathrm{N} = \sigma B_{\max}^2 L_\mathrm{c}/\rho U$, and the Péclet number $\mathrm{Pe} = U L_\mathrm{c}/\alpha$, where ν and α are the kinematic viscosity and the thermal diffusivity. The interaction parameter and the Péclet number can also be expressed as $\mathrm{N} = \mathrm{Ha}^2/\mathrm{Re}$, and $\mathrm{Pe} = \mathrm{Pr}\,\mathrm{Re}$, where $\mathrm{Ha} = B_{\max} L_\mathrm{c} \sqrt{\sigma/\rho\nu}$ and $\mathrm{Pr} = \nu/\alpha$ are the Hartmann and the Prandtl number, respectively. Eqs. (1)–(4) are, respectively, the continuity, Navier–Stokes, heat transfer, and induction equations, while

Eqs. (5) and (6) are the Ampère and magnetic Gauss laws, respectively. In the heat transfer equation (3) the viscous and Ohmic dissipation terms were omitted since are extremely small for the explored conditions.

The boundary conditions used for the numerical solution of the problem are the following. At the entrance of the duct, a constant and uniform flow $u=1$ and temperature $T=0$ are imposed. At the outlet of the duct, the streamwise gradient of velocity and temperature is set to zero to satisfy the fully developed conditions. At the duct walls, the no-slip condition for the velocity is applied, whereas the side wall at $y=L_y$ has a zero normal temperature gradient at the surface (thermally insulating wall), $\partial T/\partial y=0$, and at the side wall $y=0$ (heated wall) a constant temperature $T=1$ is fixed. The heated wall is assumed to be perfectly conducting and, therefore, the induced magnetic field must satisfy the condition $\partial b/\partial y=0$, whereas the thermally insulating wall at $y=L_y$ is also assumed electrically insulating, so that the boundary condition becomes $b=0$.

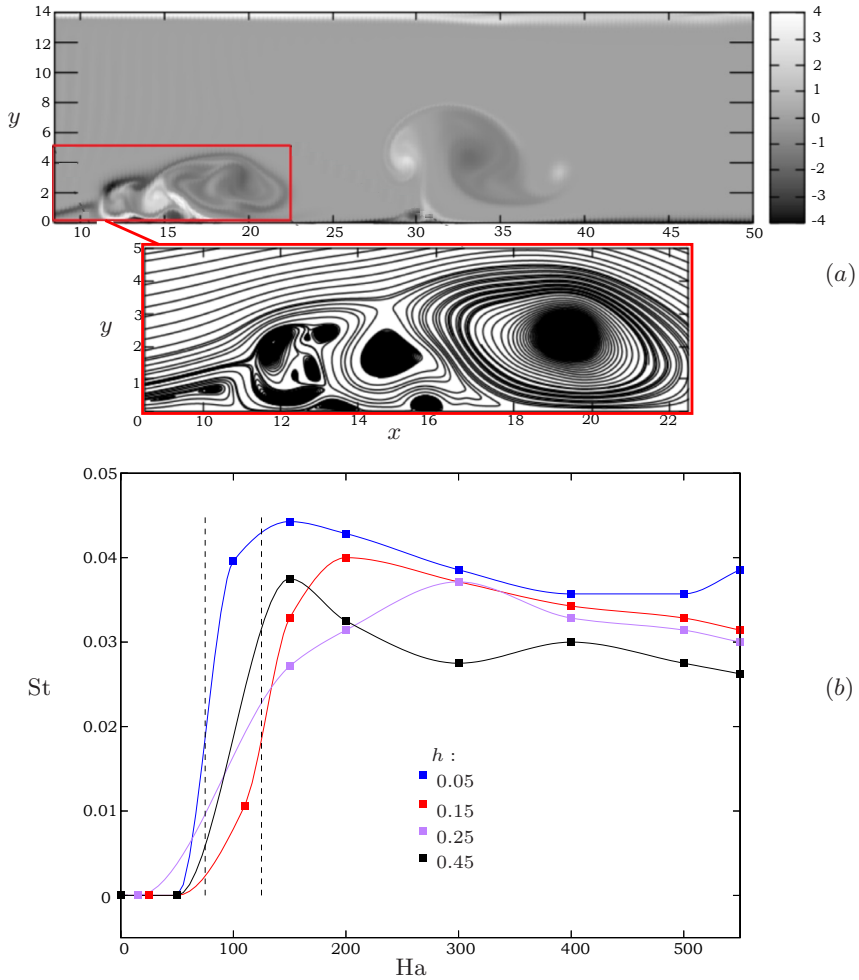

Fig. 2. (*a*) Vorticity map and streamlines of a zoomed region for $\mathrm{Re}=1000$ and $\mathrm{Ha}=250$ ($\mathrm{N}=62$) at $t=600$. (*b*) The Strouhal number St as a function of the Hartmann number Ha for different values of the gap ratio h and $\mathrm{Re}=1000$.

A finite volume code has been developed for numerical solution of the governing equations. The SIMPLEC algorithm was employed to handle the pressure–velocity coupling with a staggered regular grid. The upwind differencing scheme was applied for convective terms whereas the second-order central difference was used for diffusive terms. Time integration was performed with the first order Euler scheme. A high-resolution uniform mesh of 900×700 nodes with $\Delta x = 0.05$ and $\Delta y = 0.02$ was used, while the time step was of the order 10^{-3}. A mesh independence study was also carried out. The code validation was performed by comparing numerical results against published results and analytical solutions.

2. Flow dynamics and heat transfer analysis.

Fig. 2*a* shows the vorticity map for a given time instant for $\mathrm{Re} = 1000$, $\mathrm{Ha} = 250$, and $h = 0.15$. Additionally, a zoom of the region around the magnetic fin is also shown with streamlines, where a strong modification of the upstream flow due to its presence close to the sidewall can be clearly observed. The strength of the coupling between the electromagnetic and inertial forces ($\mathrm{N} = 62$) is enough to produce a wake downstream the high magnetic intensity region with periodic vortex detachment that produces stirring close to the hot wall. The dimensionless frequency of the vortex shedding can be observed in Fig. 2*b*, where the Strouhal number $\mathrm{St} = fL_c/U$ is plotted as a function of the Hartmann number for $\mathrm{Re} = 1000$ and several gap ratios h. It is observed that for small Ha numbers, $\mathrm{Ha} < 75$, there is no vortex shedding, whereas a transition occurs over the range between dotted lines, and the onset of vortex shedding appears at $\mathrm{Ha} \approx 150$. Depending on the gap ratio h, the Strouhal number reaches a maximum. As it will be discussed later, the onset of the vortex shedding has a direct effect on the heat transfer.

Fig. 3 shows, through snapshots, the effect of the magnetic fin on the temperature field for two cases, namely, (*a*) and (*b*) $\mathrm{Re} = 1000$, $\mathrm{N} = 5.6$, and (*c*) and (*d*) $\mathrm{Re} = 1000$, $\mathrm{N} = 84.1$. These snapshots show the instantaneous changes produced by electromagnetic stirring, particularly, how the thermal boundary layer on the sidewall is disrupted by the presence of the magnetic fin. Note that the greater agitation is observed in cases (*c*) and (*d*), where the interaction parameter is larger, leading to more widespread detached vortices. For the smaller value $\mathrm{N} = 5.6$, the cross-stream temperature gradients are reduced, which means a less intense heat flow through the wall. To investigate this in more detail,

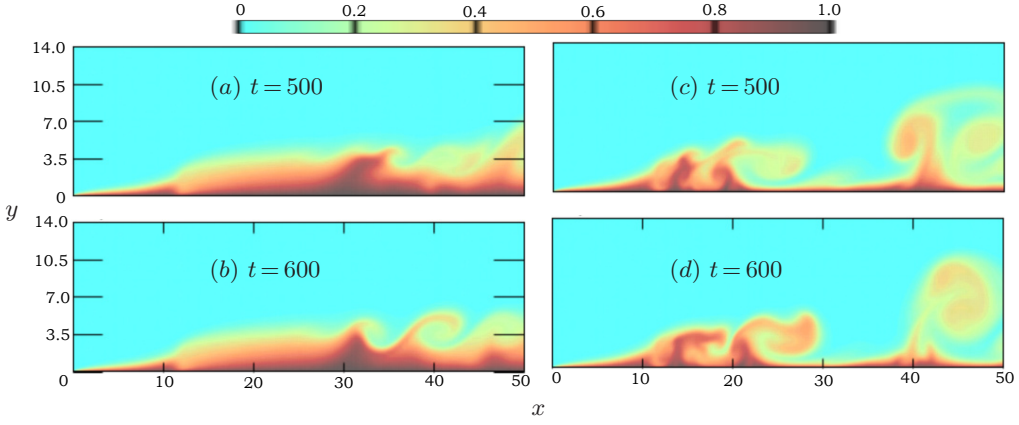

Fig. 3. Temperature field at two time instants. (*a*) and (*b*) $\mathrm{Re} = 1000$, $\mathrm{N} = 5.6$. (*c*) and (*d*) $\mathrm{Re} = 1000$, $\mathrm{N} = 84.1$.

the heat transfer enhancement was evaluated through the global Nusselt number

$$\mathrm{Nu} = \frac{1}{L_x}\int_0^{L_x} \overline{\mathrm{Nu}}_x(x)\mathrm{d}x,$$

computed by integrating over time the local Nusselt number

$$\mathrm{Nu}_x(x,t) = \left.\frac{\partial T}{\partial y}\right|_w \frac{L_y}{T_\mathrm{b} - T_\mathrm{w}},$$

along the hot wall, with T_w and T_b being the wall and bulk temperatures, the latter defined as

$$T_\mathrm{b}(x,t) = \frac{\int_0^{L_y} uT\mathrm{d}y}{\int_0^{L_y} u\mathrm{d}y}.$$

Three Reynolds numbers were explored, namely, $\mathrm{Re} = 500, 1000$ and 1500, and the Hartmann number was varied in the range $0 \leq \mathrm{Ha} \leq 550$, while the effect of the location of the magnet with respect to the heated wall was examined by considering different values of the gap ratio h, i.e. $h = 0.05, 0.15, 0.25, 0.45$. Fig. 4 shows the global Nusselt number as a function of the interaction parameter for different Reynolds numbers and the fixed $h = 0.25$ value. It is observed that for the different Re values, the maximum Nu is obtained for the same critical interaction parameter $\mathrm{N} \approx 105$. This means that the optimum Nu value is obtained for the same ratio of Lorentz to inertia forces. Moreover, the presence of the magnetic fin produces a local pressure drop due to the braking of the flow caused by the Lorentz force. Fig. 5 shows the local pressure drop calculated

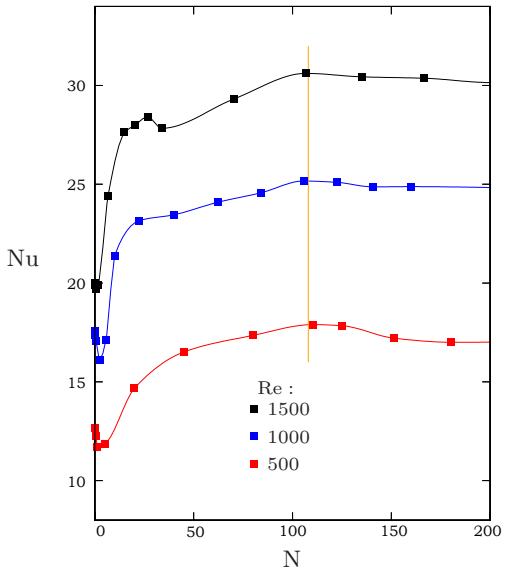

Fig. 4. The Nusselt number Nu as a function of the interaction parameter N for $\mathrm{Re} = 500, 1000$ and 1500, the gap ratio is $h = 0.25$.

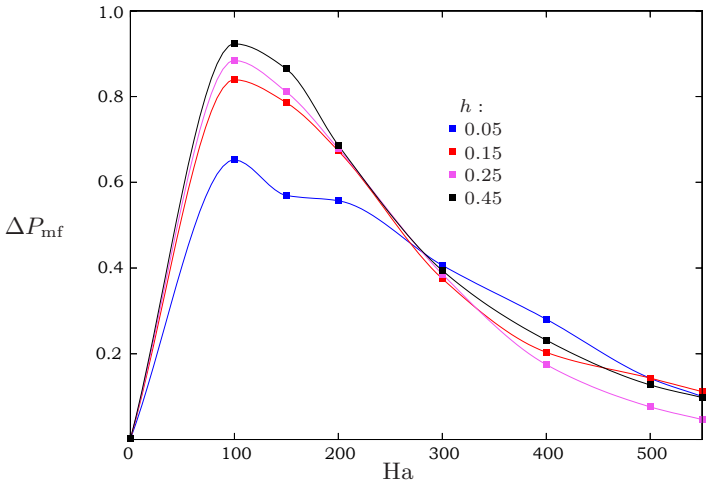

Fig. 5. Local pressure drop ΔP_{mf} as a function of the Hartmann number Ha and $\mathrm{Re} = 1000$.

upstream and downstream the magnetic fin as a function of Ha for different values of h. Note that a maximum is reached for $\mathrm{Ha} = 100$ for all h values and that it increases as h increases.

As it is usually done with mechanical swirl flow devices, the thermal performance factor η, defined as [1]

$$\eta = \frac{\mathrm{Nu}/\mathrm{Nu}_0}{(f/f_0)^{1/3}}, \tag{7}$$

can be used to evaluate the performance of the magnetic fin, where Nu_0 is the Nusselt number of the purely hydrodynamic flow, while f and f_0 are the friction factors with and without the magnetic fin. A device with a good performance is able to reach a significant increase of the heat transfer coefficient (i.e. Nu) with a minimum increase of the friction factor. The latter is calculated from the global pressure drop across the test section due to the interaction between the fluid and the duct with inserts (a magnetic fin, in this case). It was found that due to the location of the magnet and its size relative to the width of the duct, the friction factor remains practically unchanged, either with or without the magnetic fin. Fig. 6 displays η and the percentage increment of the overall heat transfer $HI = \langle(\mathrm{Nu} - \mathrm{Nu}_0)/\mathrm{Nu}_0\rangle \times 100\%$ as a function of Ha for $\mathrm{Re} = 1000$ and different h values. It is observed that for $\mathrm{Ha} < 100$ the performance of the magnetic fin is in general worse than the purely hydrodynamic flow for all values of h. This corresponds to negative percentage values of HI. Note from Fig. 2*b* that in this region of Ha values the vortex shedding has not started yet, that is, $\mathrm{St} = 0$. As Ha increases ($\mathrm{Ha} > 100$), η rises and reaches a maximum value for each value of h. It was found that for $\mathrm{Re} = 1000$ optimal conditions that maximize η occurred when $h = 0.15$ and $\mathrm{Ha} = 290$. In terms of HI, this corresponds to a maximum percentage increment 43.2 % compared to the purely hydrodynamic case. This behaviour may be explained by contrasting the inertial and Lorentz forces. For a given Re, when Ha is small, inertia overcomes the Lorentz force so that the braking of the flow is not strong enough to produce vortex shedding and boundary layer detachment, therefore, the heat transfer from the hot wall is reduced. As Ha grows, the opposing Lorentz force increases and may become comparable with

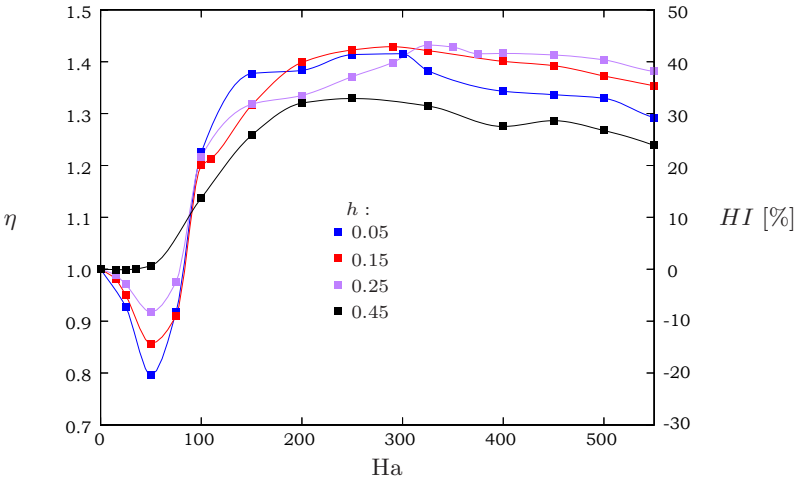

Fig. 6. Global thermal performance η, percentage increment of heat transfer HI as a function of Ha at different gap ratios h and $\mathrm{Re} = 1000$.

inertia or even much larger. In this case, vortex shedding is produced by the magnetic fin, promoting an efficient stirring near the heated wall and enhancing the heat transfer.

3. Conclusions.

Assuming a two-dimensional approximation, a numerical heat transfer characterization of the performance of a magnetic fin in a liquid metal duct flow was carried out in a wide range of Hartmann numbers for three fixed Reynolds numbers. Although this approximation strongly limits the scope of our approach, it retains some important physical features of the flow. When the coupling between electromagnetic and inertial forces is strong enough, vortex shedding arises producing an intense stirring that increases the heat transfer from the heated wall. For the Re values explored, the global Nusselt number Nu presents a maximum for $\mathrm{N} \approx 105$, what means that the optimal heat transfer is obtained for the same ratio of Lorentz to inertial forces. As the blockage ratio is small ($\beta = 1/7$), the friction factor remains practically unchanged with or without the magnetic fin, thus, the trend of the global thermal performance η and the percentage increment of heat transfer HI as functions of the Hartmann number Ha are similar. For $\mathrm{Re} = 1000$, an optimal global performance $\eta = 1.43$ or a maximum percentage of heat transfer improvement of 43% compared to the purely hydrodynamic case was obtained for a given ratio $h = 0.15$ and $\mathrm{Ha} = 290$. Therefore, magnetic fins appear to be a suitable non-intrusive method to enhance heat transfer in liquid metal duct flows and deserve to be studied in more realistic situations.

Acknowledgements.

This research was supported by CONACYT, under project no. 258623, and CONACYT-SENER-Sustentabilidad Energética under project no. 272063. A. Figueroa thanks the Investigadoras e Investigadores por México program from Conacyt.

References

[1] M. Sheikholeslami, M. Gorji-Bandpy, D.D. Ganji. Review of heat transfer enhancement methods: Focus on passive methods using swirl flow devices. *Renew. Sustain. Energy Reviews*, vol. 49 (2015), pp. 444–469.

[2] O.G. Cassells, W.K. Hussam, and G.J. Sheard. Heat transfer enhancement using rectangular vortex promoters in confined quasi-two-dimensional magnetohydrodynamic flows. *Int. J. Heat Mass Transfer*, vol. 93 (2016), pp. 186–199.

[3] M. Modestov, E. Kolemen, A.E. Fisher, M.G. Hvasta. Electromagnetic control of heat transport within a rectangular channel filled with flowing liquid metal. *Nuclear Fusion*, vol. 58 (2018), no. 1, p. 016009.

[4] A.H.A. Hamid, W.K. Hussam and G.J. Sheard. Combining an obstacle and electrically driven vortices to enhance heat transfer in a quasi-two-dimensional MHD duct flow. *J. Fluid Mech.*, vol. 792 (2016), pp. 364–396.

[5] M. Gallo, H. Nemati, B.J. Boersma *et al.* "Magnetic-ribs" in fully developed laminar liquid-metal channel flow. *Int. J. Heat Fluid Flow*, vol. 56 (2015), pp. 198–208.

[6] S. Cuevas, S. Smolentsev, and M.A. Abdou. On the flow past a magnetic obstacle. *J. Fluid Mech.*, vol. 553 (2006), pp. 227–252.

[7] X. Zhang, H. Huang. Effect of local magnetic fields on electrically conducting fluid flow and heat transfer. *J. Heat Transfer ASME*, vol. 135 2013, p. 021702.

[8] X.D. Zhang, and H.L. Huang. Heat transfer enhancement of MHD flow by a row of magnetic obstacles. *Heat Transfer Res.*, vol. 46 (2015), no. 12, pp. 1101–1121.

[9] E.P. Furlani. Permanent Magnet and Electromechanical Devices: Materials, Analysis, and Applications. (New York, Academic Press, 2001, 215 p.)

Received 09.12.2022